Tomasz RYMARCZYK[1,2]**, Piotr BOŻEK**[1]**, Michał OLESZEK**[1]**, Konrad NIDERLA**[1,2]**,**
Przemysław ADAMKIEWICZ[1,2]

Research & Development Centre Netrix S.A.(1), University of Economics and Innovation (2)

Construction of the SmartEIT tomograph based on electrical impedance tomography

Abstract. The article presents the prototype of the SmartEIT measuring device construction based on the Raspberry Pi platform using electric impedance tomography. The measurement with the device consists in placing electrodes on the tested object, two electrodes are connected to alternating current, and the voltage drop is measured on the other. SmartEIT enables measurements on 16 electrodes. The electrodes can be made of copper without a shield or covered with conductive rubber, depending on the tested object. In each cycle, SmartEIT forces AC flow with a sinusoidal waveform with a constant amplitude and a frequency of 1 kHz between the two farthest electrodes. The current is relatively low, selected during measurements so that the capacity of the power source is not exceeded.

Streszczenie. W artykule przedstawiono prototyp konstrukcji urządzenia pomiarowego SmartEIT oparty na platformie Raspberry Pi z wykorzystaniem elektrycznej tomografii impedancyjnej. Pomiar za pomocą urządzenia polega na umieszczeniu elektrod na badanym obiekcie, dwie elektrody są podłączone do prądu przemiennego, a spadek napięcia jest mierzony na pozostałych. SmartEIT umożliwia wykonywanie pomiarów na 16 elektrodach. Elektrody mogą być wykonane z miedzi bez osłony lub pokryte gumą przewodzącą, w zależności od badanego obiektu. W każdym cyklu SmartEIT wymusza przepływ prądu przemiennego sinusoidalnym przebiegiem o stałej amplitudzie i częstotliwości 1 kHz między dwiema najdalszymi elektrodami. Natężenie prądu jest stosunkowo niskie, wybrane podczas pomiarów, tak aby wydajność źródła prądu nie została przekroczona. (Budowa tomografu SmartEIT w oparciu o platformę Raspberry Pi).

Keywords: electrical impedance tomography, sensors.
Słowa kluczowe: elektryczna tomografia impedancyjna, sensory.

Introduction

Electrical tomography provides a non-invasive technique and non-destructive technique, in contrast to many others (like chemical methods) for measuring different kinds of objects and problems. In this method, a power or voltage source is connected to the object, and then a current distribution or voltage distribution on the edge of the object is observed. The collected information is processed by an algorithm that reconstructs the image [1-15].

SmartEIT is a prototype of a miniature tomograph cooperating with the Raspberry Pi platform. The device in the form of a plug directly attached to Raspberry does not require an additional power supply [1]. Many different methods are used to solve optimization problems [16-29]. The solution was based on electrical impedance tomography [30-37].

Measurements

A set of electric currents are sent through the examined object through these electrodes, and the obtained voltages are measured using the same electrodes. Figure 1 shows the opposite method of acquiring boundary potential data illustrated for a cylindrical volumetric guide and 16 equally spaced electrodes: (a) first projection-1, (b) second projection-2. Due to the unknown value of the voltage drops between the tested object and the electrodes to which the electric current source (I) is connected, these electrodes are not taken into account during the measurements. For each projection angle 12 independent voltage measurements (V) may be obtained between individual pairs of adjacent electrodes. For a system with 16 electrodes (we labelled them as variable *n*), there are 16 possibilities to connect the power source, but because of the symmetry of the system, only half of them (*n* / 2 = 8) are accepted. Input data for the image construction algorithm are voltage measurements made between adjacent electrodes. Measurements made using electrodes with an attached excitation source are omitted due to the unknown voltage drop between these electrodes and the tested area. For a system of n = 16 electrodes and any projection angle, n - 3 = 12 independent measurements may be obtained. Thus, the full number of voltages measurable between neighbouring voltage electrodes at n / 2 = 8 angles is: (n - 3) (n / 2) = 12 · 8 = 96. The method used to measure the inter-electrode voltages corresponds to the first and the second projection angle. For subsequent angles, the sequential switching of the power supply and measurement circuit to the neighbouring electrodes takes place.
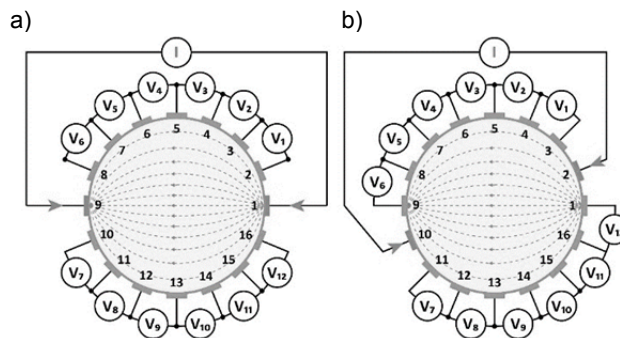

Fig. 1. Opposite measurement method in a system of 16 electrodes: a) first measuring cycle, b) next measurement cycle.
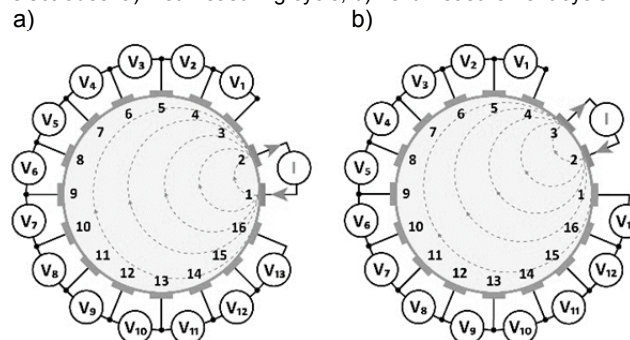

Fig.. 2. Neighbouring measurement method in a system of 16 electrodes: a) first measuring cycle, b) next measurement cycle.

Figure 2 presents the neighbouring (adjacent current method) of boundary potential data collection illustrated for a cylindrical volume conductor and 16 equally spaced

electrodes: (a) first projection-1, (b) second projection-2.The boundary potential data collection for collecting data from potential measurements at the edge of an object using 16 electrodes was shown in Fig. 3. In the opposite current injection method, the current is injected through two diametrically opposed electrodes in each current projection and the potentials are measured on all the electrodes with respect to the ground point of the analog electronics. In the other method, the current is applied through neighbouring electrodes the potentials are measured on all the electrodes with respect to the ground point of the analog electronics.
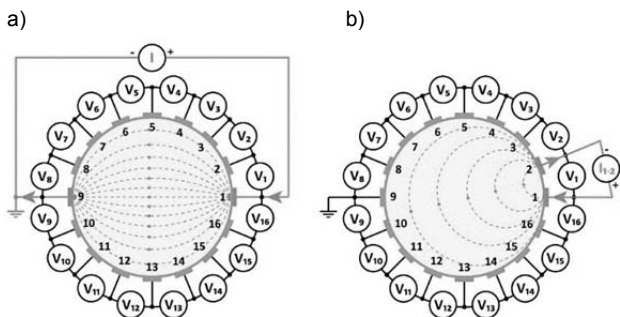

Fig. 3.Boundary potential data collection - measurement model in electrical impedance tomography: a) opposite, b) neighbouring method.

SmartEIT device

SmartEIT enables visual measurements on 16 electrodes. A compact device the size of a credit card due to the use of a highly efficient converter increasing the DC / DC voltage has a voltage of 30 Vpp necessary for forcing the flow of current in high impedance facilities, even though it is powered directly from the Raspberry (5 V) Platform. A set of passive electrodes is needed to perform the measurements.
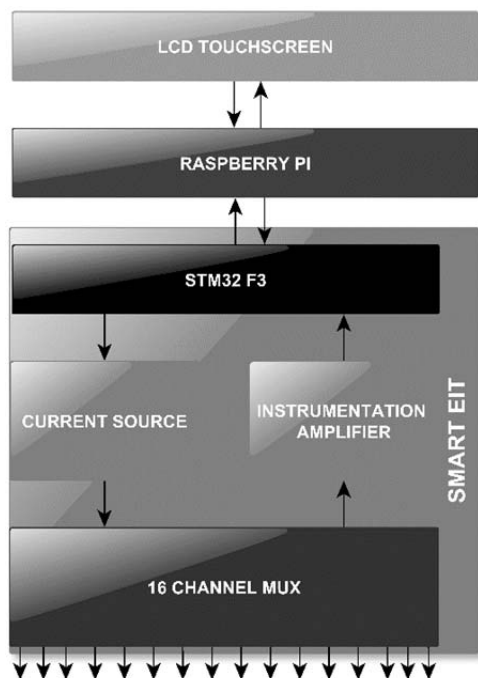

Fig. 4. Block diagram of the set.

The electrodes can be made of copper without a shield or covered with conductive rubber, depending on the tested object. The measurements are carried out with the help of sixteen electrodes applied to the tested object. One complete measurement is made in sixteen cycles. In each cycle,
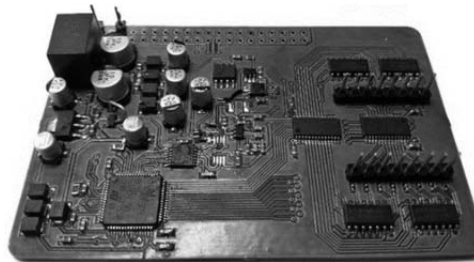

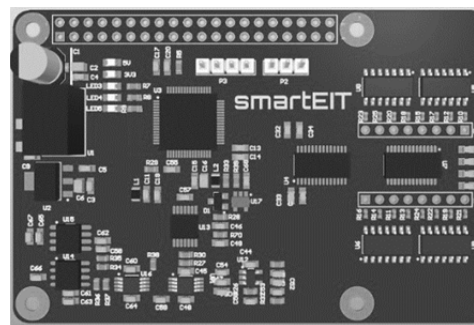Fig. 5. Diagram of the measuring block.

Fig. 6. Test version of the device.

Fig. 7. The Smart EIT device.

SmartEIT forces AC flow with a sinusoidal waveform with a constant amplitude and a frequency of 1 kHz between the two farthest electrodes. The current is relatively low, e.g. 100uA, selected during measurements so that the capacity of the power source is not exceeded. During the current flow, the voltages occurring on the remaining electrodes occur sequentially. The measurement is always carried out in relation to one of the force electrodes with which the mass is connected. In subsequent cycles, the current forcing is transferred to the following pairs of electrodes. The result of the full measurement is a matrix consisting of 244 voltage values that are sent via the SPI interface to the Raspberry Pi. The Raspberry development board does not take active part in measurements, it is only used to process ready data. After

connecting the LCD display it will be possible to obtain simple reconstructions without using a computer.
Measuring block

After passing through the multiplexer, the received signals are sent to a measuring block consisting of an active high-pass filter cutting off frequencies below 1 kHz, an INA826 measuring amplifier with adjustable gain and a protective circuit of the analog-to-digital converter. Gain adjustment is done using an 8-bit digital MCP41HV5 potentiometer connected to an amplifier controlled by the SPI interface via a microcontroller. The last element of the block is the sigma-delta analog-to-digital converter. There is a 16-bit converter with a conversion rate of up to 50ksps. This system has 7 gain levels.

Methods and Models

The so-called Generalized Tikhonov regularization is very often used in electrical impedance tomography for image reconstruction. In the literature on the subject, this method is also known as the Gauss-Newton algorithm (GN) in the generalized form. In order to carry out quantitative considerations, it may be assumed that the tested object is polarized with low-frequency current. Then, the electrical material properties can be described by a function with real values. In this case, in the generalized Laplace equation, the term proportional to the frequency is neglected, and this function can be identified with the real isotropic admittivity case. The measurement objects and the image reconstructions were shown in Fig. 8-9.
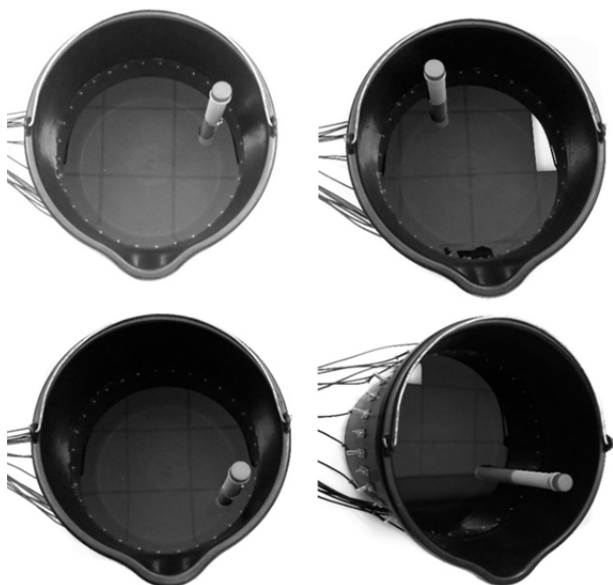

Fig. 8. Measuring object.

The reconstruction of the interior image of the object under investigation is connected with the determination of the global minimum of the objective function, which in the case under consideration is defined as follows:

$$(1) \quad F(\gamma) = \frac{1}{2}\left\{ \left\| \mathbf{L}_1 \left(\mathbf{U}_m - \mathbf{U}_s(\gamma) \right) \right\|^2 + \lambda^2 \left\| \mathbf{L}_2 \left(\gamma - \gamma^* \right) \right\|^2 \right\}$$

where: γ – conductivity vector, γ^* - conductivity vector adopted a priori - it represents known properties of the interior of the object, $\mathbf{U}_m$ - voltages obtained as a result of the measurements, $\mathbf{U}_s(\gamma)$ - voltages received by numerical calculations (FEM), $\mathbf{L}_1$ - square matrix, $\mathbf{L}_2$ - regularization matrix, it is usually a unit matrix. It can also provide a discreet approximation of the selected differential operator. λ - regularization parameter - positive real number.

Using appropriate approximations, it can be demonstrated that the conductivity proper in the iteration denoted by k + 1 is given by the following formula:

$$(2) \quad \gamma_{k+1} = \gamma_k + \alpha_k \left(\mathbf{J}_k^T \mathbf{W}_1 \mathbf{J}_k + \lambda^2 \mathbf{W}_2 \right)^{-1} \left[\mathbf{J}_k^T \mathbf{W}_1 \left(\mathbf{U}_m - \mathbf{U}_s(\gamma_k) \right) - \lambda^2 \mathbf{W}_2 \left(\gamma_k - \gamma^* \right) \right] (2)$$

where: $\mathbf{J}_k = \left[\frac{\partial U_s(\gamma)}{\partial \gamma} \right]_{\gamma=\gamma_k}$; $\mathbf{W}_1 = \mathbf{L}_1^T \mathbf{L}_1$; $\mathbf{W}_2 = \mathbf{L}_2^T \mathbf{L}_2$; $\mathbf{J}_k$ - Jacobian matrix calculated in the k-th step, $\mathbf{W}_1$ - weighting matrix - it is usually a unit matrix, α_k - step length.
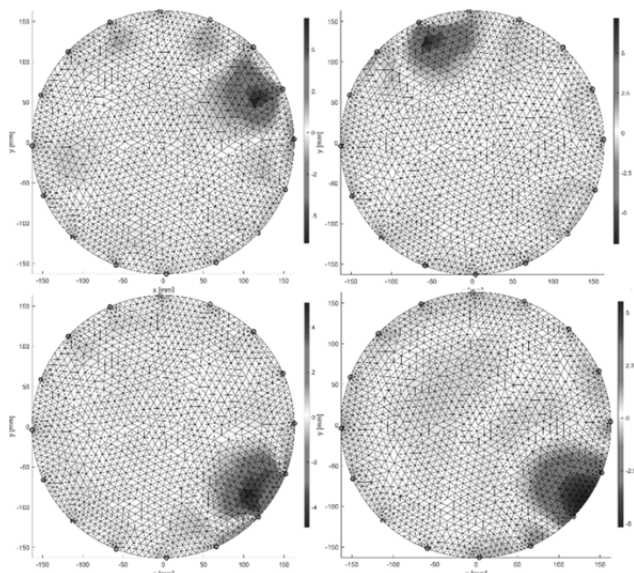

Fig. 9. Image reconstruction - Gauss-Newton method

Conclusion

The paper presents the construction of the SmartEIT measuring device based on electric impedance tomography. The presented solution works with the Raspberry Pi platform. The measurement by the device consists in placing electrodes on the tested object and measuring on the remaining ones. SmartEIT enables visual measurements on 16 electrodes. In each cycle, the device forces AC flow with a sinusoidal waveform with a constant amplitude and a frequency of 1 kHz between the two farthest electrodes. The current is relatively low, selected during measurements so that the capacity of the power source is not exceeded. The effectiveness of the measurements was verified by the Gauss-Newton method, which was used to solve the inverse problem.

Authors: Tomasz Rymarczyk, Ph.D. Eng., University of Economics and Innovation, Projektowa 4, Lublin, Poland/ Research & Development Centre Netrix S.A. E-mail: tomasz@rymarczyk.com; Piotr Bożek, Research & Development Centre Netrix S.A., E-mail:piotr.bozek@netrix.com.pl; Michał Oleszek, Research & Development Centre Netrix S.A., E-mail: michal.oleszek@netrix.com.pl; Konrad Niderla, University of Economics and Innovation, Projektowa 4, Lublin, Poland/ Research & Development Centre Netrix S.A. E-mail: konrad.niderla@netrix.com.pl; Przemysław Adamkiewicz, Ph.D., University of Economics and Innovation, Projektowa 4, Lublin, Poland/ Research & Development Centre Netrix S.A. E-mail: p.adamkiewicz@netrix.com.pl;

REFERENCES
[1] Bozek P., Rymarczyk T., Oleszek M., Adamkiewicz P., Prototype of miniature electrical impedance tomograph SmartEIT cooperating with raspberry Pi platform 2019

Applications of Electromagnetics in Modern Engineering and Medicine, PTZE 2019, 2019, 17-21.

[2] Beck M. S., Byars M., Dyakowski T., Waterfall R., He R., Wang S. J., Yang W. Q., Principles and Industrial Applications of Electrical Capacitance Tomography, Measurement and Control, September, 30 (1997), No. 7.

[3] Chaniecki Z., Romanowski A., Nowakowski J., Niedostatkiewicz M., Application of twin-plane ECT sensor for identification of the internal imperfections inside concrete beams Grudzien, IEEE Instrumentation and Measurement Technology Conference, 2016, 7520512.

[4] Grudzien K., Romanowski A., Chaniecki Z., Niedostatkiewicz M., Sankowski D., Description of the silo flow and bulk solid pulsation detection using ECT, Flow Measurement and Instrumentation, 21 (2010), No. 3, 198-206.

[5] Kryszyn J., Wanta D. M., Smolik W. T., Gain Adjustment for Signal-to-Noise Ratio Improvement in Electrical Capacitance Tomography System EVT4, IEEE Sens. J., 17 (2017), No. 24, 8107–8116.

[6] Kryszyn J., Smolik W., Toolbox for 3d modelling and image reconstruction in electrical capacitance tomography, Informatyka, Automatyka, Pomiary w Gospodarce i Ochronie Środowiska (IAPGOŚ) , 7 (2017), No. 1, 137-145.

[7] Majchrowicz M., Kapusta P., Jackowska-Strumiłło L., Sankowski D., Acceleration of image reconstruction process in the electrical capacitance tomography 3d in heterogeneous, multi-gpu system, Informatyka, Automatyka, Pomiary w Gospodarce i Ochronie Środowiska (IAPGOŚ) , 7 (2017), No. 1, 37-41.

[8] Nowakowski J., Ostalczyk P., Sankowski D., Application of fractional calculus for modelling of two-phase gas/liquid flow system, Informatyka, Automatyka, Pomiary w Gospodarce i Ochronie Środowiska (IAPGOŚ) , 7 (2017), No. 1, 42-45.

[9] Romanowski A., Big Data-Driven Contextual Processing Methods for Electrical Capacitance Tomography, in IEEE Transactions on Industrial Informatics, 15 (2019), No. 3, 1609-1618.

[10] Rymarczyk T, Kłosowski G. Innovative methods of neural reconstruction for tomographic images in maintenance of tank industrial reactors. Eksploatacja i Niezawodnosc – Maintenance and Reliability, 21 (2019); No. 2, 261–267

[11] Rymarczyk, T.; Kozłowski, E.; Kłosowski, G.; Niderla, K. Logistic Regression for Machine Learning in Process Tomography, Sensors, 19 (2019), 3400.

[12] Rymarczyk T., Adamkiewicz P., Polakowski K., Sikora J., Effective ultrasound and radio tomography imaging algorithm for two-dimensional problems, Przegląd Elektrotechniczny, 94 (2018), No 6, 62-69

[13] Soleimani M., Mitchell CN, Banasiak R., Wajman R., Adler A., Four-dimensional electrical capacitance tomography imaging using experimental data, Progress In Electromagnetics Research, 90 (2009), 171-186.

[14] Smolik W., Kryszyn J., Olszewski T., Szabatin R., Methods of small capacitance measurement in electrical capacitance tomography, Informatyka, Automatyka, Pomiary w Gospodarce i Ochronie Środowiska (IAPGOŚ) , 7 (2017), No. 1, 2017, 105-110.

[15] Wajman R., Fiderek P., Fidos H., Sankowski D., Banasiak R., Metrological evaluation of a 3D electrical capacitance tomography measurement system for two-phase flow fraction determination, Measurement Science and Technology, 24 (2013), No. 6, 065302.

[16] Dušek J., Hladký D., Mikulka J., Electrical Impedance Tomography Methods and Algorithms Processed with a GPU, In PIERS Proceedings, 2017, 1710-1714.

[17] Goetzke-Pala A., Hoła J., Influence of burnt clay brick salinity on moisture content evaluated by non-destructive electric methods. Archives of Civil and Mechanical Engineering., 16 (2016), No. 1, 101-111.

[18] Kłosowski G., Kozłowski E., Gola A., Integer linear programming in optimization of waste after cutting in the furniture manufacturing, Advances in Intelligent Systems and Computing 2018; 637 (2018), 260-270.

[19] Kozlowski E., Mazurkiewicz D., Kowalska B., et al., Binary Linear Programming as a Decision-Making Aid for Water Intake Operators, 1st International Conference on Intelligent Systems in Production Engineering and Maintenance (ISPEM), Wroclaw, Poland, Sep 28-29.2017, Book Series: Advances in Intelligent Systems and Computing, 637 (2018), 199-208.

[20] Krawczyk A., Korzeniewska E., Łada-Tondyra, E. Magnetophosphenes – History and contemporary implications, Przeglad Elektrotechniczny, 94 (2018), No 1, 61-64.

[21] Korzeniewska E., Walczak M., Rymaszewski J., Elements of Elastic Electronics Created on Textile Substrate, Proceedings of the 24th International Conference Mixed Design of Integrated Circuits and Systems - MIXDES 2017, 2017, 447-45.

[22] Lopato P., Herbko M., A Circular Microstrip Antenna Sensor for Direction Sensitive Strain Evaluation, Sensors, 18 (2018), No. 1, 310.

[23] Psuj G., Multi-Sensor Data Integration Using Deep Learning for Characterization of Defects in Steel Elements, Sensors, 18 (2018), No. 1, 292.

[24] Szczęsny A., Korzeniewska E., Selection of the method for the earthing resistance measurement, Przegląd Elektrotechniczny, 94 (2018), No. 12, 178-181.

[25] Valis D., Mazurkiewicz D., Application of selected Levy processes for degradation modelling of long range mine belt using real-time data, Archives of Civil and Mechanical Engineering, 18 (2018), No. 4, 1430-1440.

[26] Ren S., Soleimani M., Xu Y., Dong F., Inclusion boundary reconstruction and sensitivity analysis in electrical impedance tomography, Inverse Problems in Science and Engineering, 26 (2018), No. 7, 1037-1061

[27] Kozłowski E., Mazurkiewicz D., Żabiński T., Prucnal S., Sęp J., Assessment model of cutting tool condition for real-time supervision system, Eksploatacja i Niezawodnosc – Maintenance and Reliability, 21 (2019); No 4, 679–685

[28] Vališ D, Hasilová K., Forbelská M, Vintr Z, Reliability modelling and analysis of water distribution network based on backpropagation recursive processes with real field data, Measurement 149 (2020), 107026

[29] Kowalska A., Banasiak R., Romanowski A., Sankowski D., Article 3D-Printed Multilayer Sensor Structure for Electrical Capacitance Tomography, 19 (2019), Sensors, 3416

[30] Adler A., Lionheart W., Uses and abuses of EIDORS: An extensible software base for EIT, Phys. Meas., 27 (2006), 25–42.

[31] Borcea L, Electrical impedance tomography, Inverse Problems, 18 (2002), 99–136.

[32] Holder D., Introduction to biomedical electrical impedance tomography Electrical Impedance Tomography Methods, History and Applications, Bristol, Institute of Physics, 2005.

[33] Kłosowski G., Rymarczyk T., Gola A., Increasing the reliability of flood embankments with neural imaging method. Applied Sciences, 8 (2018), No. 9, 1457.

[34] Rymarczyk T., Szumowski K., Adamkiewicz P., Tchórzewski P., Sikora J., Moisture Wall Inspection Using Electrical Tomography Measurements, Przegląd Elektrotechniczny, 94 (2018), No 94, 97-100

[35] Duda K., Adamkiewicz P., Rymarczyk T., Niderla K., Nondestructive Method to Examine Brick Wall Dampness, International Interdisciplinary PhD Workshop Location: Brno, Czech Republic Date: SEP 12-15, 2016, 68-71

[36] Wang M., Industrial Tomography: Systems and Applications, Elsevier, 2015